Available online at www.sciencedirect.com
ScienceDirect
Journal of the European Ceramic Society 27 (2007) 73–78
www.elsevier.com/locate/jeurceramsoc

Microstructure evaluation of MgO–C refractories with TiO_2- and Al-additions

C.G. Aneziris, J. Hubálková *, R. Barabás

Institute of Ceramic, Glass and Construction Materials, Technical University of Freiberg, Germany

Received 5 November 2005; received in revised form 13 March 2006; accepted 17 March 2006
Available online 3 May 2006

Abstract

The effect of TiO_2- and Al-additions on the oxidation resistance and the mechanical properties of MgO–C refractories is evaluated in terms of a phase evolution as a function of the coking temperature. The formation of TiCN and TiC crystalline phases in the bonding matrix contributes to superior mechanical, thermal and chemical properties of carbon-bonded refractories.

Keywords: Refractories; MgO; Mechanical properties; Oxidation resistance

1. Introduction

Magnesia–carbon bricks are established high duty refractory products with unique mechanical, thermal and chemical properties for applications in converters, electric arc furnaces and steel treatment ladles. In recent years the composition of high-duty magnesia–carbon bricks has been improved, especially in terms of the binders and additives used for better thermo-mechanical properties under ecological and economical aspects.[1,2] By using artificial resins – as alternative environmental friendly products against tar pitch bonded products – a higher isotropic glassy phase with lower oxidation resistance and more brittle bonding is obtained.[3] In order to decrease this "brittle behaviour" and increase the oxidation resistance environmental friendly artificial tar pitch binders as additions or as main binder parts are used.[4,5]

The oldest used organic binder in the production of magnesia–carbon bricks is coal-tar pitch. Its benefits include good adhesion to the granules, plastic deformability at low temperatures (low softening point for improved wetting), a high yield of coke with an anisotropic structure and low costs. A major drawback of this product is its content of carcinogenic aromatics, notably benzo[a]pyrene. Coal-tar pitches contain 10,000–13,000 ppm benzo[a]pyrene.

Hardenable artificial resins, especially phenolic resins, are an environment-friendly alternative to benzo[a]pyrene rich coal-tar pitch and are the most frequently used organic binder in the production of magnesia–carbon bricks. They can be mixed with the refractory granular materials without warming. The coke residue is similar to pitch, approximately 50%. A problem is the isotropic phase of the coke residue resulting from resins leading to more oxidation, corrosion and thermo-mechanical sensitiveness.

On the other hand, there is a relatively new Carbo-resin product (CARBOnaceous RESin), which is a high melting coal-tar resin. Although it is produced out of coal it contains extremely low carcinogenic aromatics, especially the benzo[a]pyrene (<300 ppm). After coking it forms, in contrast to resins, a highly oriented graphite-like carbon structure.

Another approach for improving the properties of resin bonded refractories deals with the application of antioxidants. Antioxidants act as inhibitors of carbon oxidation by reducing CO to C. In MgO–C refractories, metal antioxidants such as Al, Si, Mg or carbide based antioxidants such as B_4C and SiC are often used to improve the oxidation resistance on the one hand and the mechanical strength on the other hand.[6–9] With Al additions, Zhang et al.[9] observe in MgO–C fired samples at 1200 °C Al_4C_3 and Al_2O_3 located presumably at the site of the original Al metal. Some of these centres consist of an Al_2O_3 shell surrounding an Al_4C_3 core; others are solid Al_4C_3 and others are an Al_2O_3 shell containing Al particles. Besides Al_4C_3 and Al_2O_3, aluminium nitride (AlN) whiskers are formed between

* Corresponding author.
E-mail address: jana.hubalkova@ikgb.tu-freiberg.de (J. Hubálková).

0955-2219/$ – see front matter © 2006 Elsevier Ltd. All rights reserved.
doi:10.1016/j.jeurceramsoc.2006.03.001

Table 1
Compositions I, II and III

Material	Composition I		Composition II		Composition III	
	wt.%	(g)	wt.%	(g)	wt.%	(g)
MgO 2–4 mm	20.50	615.00	20.16	604.80	20.16	604.80
MgO 1–2 mm	32.50	975.00	32.43	972.90	32.43	972.90
MgO 0–1 mm	22.00	660.00	21.91	657.30	21.91	657.30
MgO (powder)	13.00	390.00	13.15	394.50	13.15	394.50
Graphite 70–150 μm	12.00	360.00	11.95	358.50	11.95	358.50
TiO_2 < 1 μm	–	–	0.40	12.00	0.40	12.00
Related to 3000 g						
Aluminum 45–75 μm	2.50	75.00	–	–	2.50	75.00
Novolak (resin)	2.20	66.00	2.20	66.00	2.20	66.00
Hexa (additive of the resin)	0.22	6.60	0.22	6.60	0.22	6.60
Carbores (coal-tar resin)	1.00	30.00	1.00	30.00	1.00	30.00

the graphite flakes and on Al_4C_3 grain surfaces. At this temperature, cuboidal spinel is occasionally observed. At a firing temperature of 1500 °C the microstructure is similar to that at 1200 °C, although little Al remains unreacted and more spinel is formed.

Lee and Duh[10] have studied reactions between MgO–C–Al refractories in contact with high-aluminium-content alloy steels. They report, in the case of Al additions in MgO–C refractories, $MgAl_2O_4$ and Al_4C_3 phases are observed in the refractory bulk, and a large amount of protective $MgAl_2O_4$ phase is formed due to the decomposition of Al_4C_3 phases on the refractory-metal reaction interface. Further the oxygen partial pressure is substantially reduced by the presence of graphite in the MgO–C–Al brick during high-temperature tests. This results in the partial nitridation of aluminium in molten high-aluminium-content alloy steel. White aluminium nitride (AlN) with the shape of whiskers is formed and adheres to the surface of the MgO–C–Al brick. Aluminium is depleted from the alloy by nitridation or the oxidation reaction by CO gas.

The effect of refractory oxides on the oxidation resistance of graphite and amorphous carbon is investigated by Yamaguchi et al.[11] Al_2O_3 accelerates the oxidation of graphite greatly. In the contrast TiO_2, ZrO_2 and MgO inhibit the oxidation of graphite. According to them TiO_2 and ZrO_2 donate electrons to graphite and stabilise its structure. Because of the existence of many defects and weaker carbon–carbon bonds, the oxidation of amorphous carbon is not effected by refractory oxides.

In the present work the interactions and the phase evolution between a commercial available binder system based on liquid phenolic resin and a powder high melting coal-tar resin with TiO_2- and Al-additions are investigated by employing X-ray diffraction (XRD), scanning electron microscope (SEM), energy dispersive X-ray (EDX) and electron backscatter diffraction EBSD techniques. In a further step, the mechanical properties and the oxidation resistance of MgO–C refractories with TiO_2- and Al-additions are studied in terms of the cold compression strength, the open porosity after coking and the oxidation depth after 3 h at 1200 °C in air atmosphere in a special furnace device.

2. Experimental

Commercially available high quality fused magnesia with a bulk density of 3.52 g/cm^3 (Possehl, Germany) and natural graphite flakes containing 94% carbon with a specific surface area of 1 m^2/g (Graphit Kropfmühl, Germany) were used as raw materials. The liquid Novolak resin (Hexion Specialty Chemicals, Germany) and powder CARBORES high melting coal-tar resin (Rütgers, Germany) were used as binders, titania powder (Tronox, Germany) and aluminium powder (TLS Technik, Germany) as additives. Table 1 shows three compositions with different TiO_2- and Al-additions (the binder system, i.e. ratio of liquid Novolak resin and powder CARBORES coal-tar resin, is identical for all three compositions).

In a first step, model-compositions without magnesia grains and graphite flakes were produced. Both binders are hand-mixed with the TiO_2- and/or the Al-addition and placed in an alumina crucible. The crucibles with the model-compositions were filled with carbon powder in order to inhibit the oxidation and covered with an alumina plate before coking at temperatures between 1000 and 1500 °C for 1 h. The phase evolutions of the model-compositions were examined in air atmosphere (all compositions) and in argon atmosphere (composition I) as a function of the coking temperature.

In the second step, all raw materials and additives according to Table 1 were mixed at room temperature following the standard commercial practice. After mixing, cylindrical samples (50 mm in diameter and 50 mm in height) were pressed (maximum pressure of 150 MPa). After pressing, the samples were cured following the standard temperature–time curve up to 180 °C. The coking of the cylindrical samples was carried out at 1000 °C for 2 h in a retort filled with carbon grit.

The open porosity and the cold compression strength (CCS) were determined following to EN 993, part 1 and part 5, respectively. The oxidation tests took place in a special electric furnace with controlled air support (10 l/min). Samples of all compositions were placed on a rotating disc and treated at 1200 °C for 3 h. The oxidation depth was measured on the cross section at three different positions. All experiments have been carried out with five samples from each composition. Table 5 show the average values and standard deviations of open poros-

Table 2
Phase evolution at 1000 °C of the model-compositions without MgO and graphite

Model compositions	C*	Al	Al_2O_3	AlN	TiO_2	TiC	TiCN	Al_4C_3	Al_2OC	Al_4O_4C	Al_2Ti_4C
I	+	+	+	–	–	–	–	+	+	–	–
II	+	–	–	–	+	–	–	–	–	–	–
III	+	+	+	–	–	+	–	+	+	–	+

C*: graphite.

Table 3
Phase evolution at 1300 °C of the model-compositions without MgO and graphite

Model compositions	C*	Al	Al_2O_3	AlN	TiO_2	TiC	TiCN	Al_4C_3	Al_2OC	Al_4O_4C	Al_2Ti_4C
I	+	–	+	–	–	–	–	+	+	+	–
II	+	–	–	–	+	–	+	–	–	–	–
III	+	–	+	–	–	+	–	+	+	+	–

C*: graphite.

ity, cold compression strength and oxidation depth for all three compositions.

3. Results and discussion

Tables 2–4 present the phase evolution due to XRD of the model-compositions I (only with Al-addition), II (only with TiO_2-addition) and III (with Al- and TiO_2-additions) coked at 1000, 1300 and 1500 °C in air and sealed by carbon in an alumina crucible. In model-compositions I and III, Al contributes to early formation of higher amounts of graphite (higher graphite peaks due to XRD already below 1000 °C) in comparison to composition II. Above 1300 °C no Al can be detected by XRD. No AlN can be identified due to XRD (negligible amount) but AlN can be observed at the grain boundaries of the Al grains at the interface carbon matrix/Al-grain by means of EDX and EBSD analysis, Figs. 2 and 3.

In the case of composition I coked at 1000 °C in air, Al_4C_3 and Al_2OC whiskers can be identified in the previous position of aluminium grains. The Al_4C_3 as well as the Al_2OC have been registered due to XRD, see also Fig. 1. According to Figs. 2 and 3 and especially Fig. 4 at higher coked temperatures amorphous whiskers containing Al, C and O due to EDX are registered. With the aid of the EBSD, no Kikuchi line patterns can be identified (no evidence of crystals) when the whiskers of Fig. 4 are examined. Further according to composition I but also III at higher coking temperatures and especially above 1300 °C also Al_4O_4C can be additionally detected. Very interesting results are demonstrated in Figs. 5 and 6. When model-composition I is coked at 1000 °C in argon and sealed by carbon in an alumina crucible Al_4C_3 crystal grains are identified and remain stable

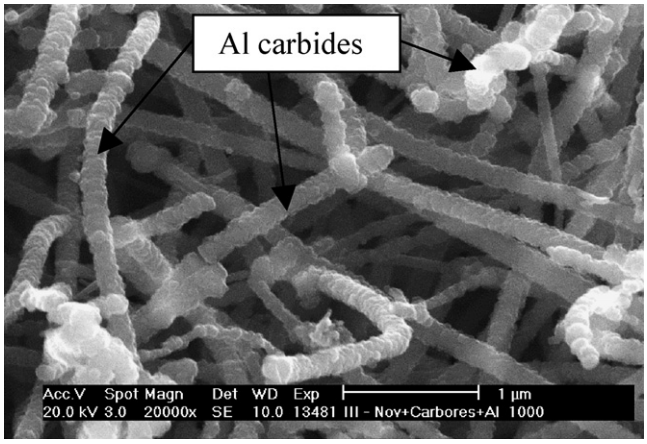

Fig. 1. Model-composition I, magnification 200,000×, coked at 1000 °C in air and sealed by carbon in an alumina crucible, whiskers based on Al_4C_3 and Al_2OC in the previous position of aluminium grains.

up to 1500 °C. According to Table 3, the model-composition III leads at 1000 °C to the formation of Al_2Ti_4C, a phase that is not stable at higher coking temperatures. Very interesting is the evidence that due to the combination of TiO_2 and Al additions mostly Al_4C_3, Al_2OC and Al_4O_4C crystalline whiskers are formed, Figs. 7 and 8. These phases remain stable and keep their crystal structure up to higher coking temperatures (in this work up to 1500 °C). Very interesting appears the shape of these whiskers; they present a dumbbell-shaped structure. It is not difficult to assume that improved properties can be achieved if straight and dumbbell-shaped nano sized carbide whiskers are well distributed in the matrix. A more flexible structure with superior thermal shock performance can be designed.

Table 4
Phase evolution at 1500 °C of the model-compositions without MgO and graphite

Model compositions	C*	Al	Al_2O_3	AlN	TiO_2	TiC	TiCN	Al_4C_3	Al_2OC	Al_4O_4C	Al_2Ti_4C
I	+	–	+	–	–	–	–	+	+	+	–
II	–	–	–	–	–	–	+	–	–	–	–
III	+	–	+	–	–	+	–	+	+	+	–

C*: graphite.

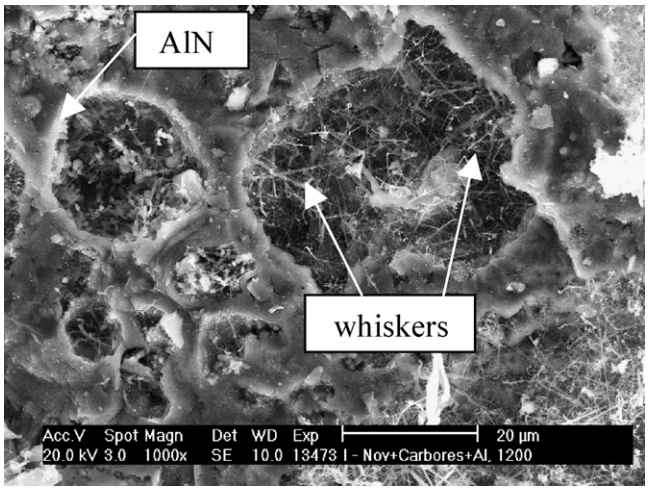

Fig. 2. Model-composition I, magnification 1000×, coked at 1200 °C in air and sealed by carbon in an alumina crucible, whiskers based on Al_4C_3 and Al_2OC and amorphous whiskers containing Al, C, O in the previous position of aluminium grains, at the interface carbon matrix/aluminium grain a mostly dense AlN layer.

In a previous work the formation of dumbbell-shaped β-SiC whiskers in Al_2O_3–ZrO_2–C composite refractories has been studied, whereby a high amount of Si has been used.[12] This has to be taken under consideration because of the interactions of steel with Si. In this work Si- and SiO_2-free dumbbell-shaped whiskers have been developed. In addition composition III contains cubic TiC already from 1000 °C in air. Higher XRD peaks of TiC can be registered at 1500 °C. In case of the model-composition II up to 1200 °C no TiC or TiCN is produced. At 1300 °C in air cubic TiCN can be detected and non reacted TiO_2. At 1500 °C only TiCN can be detected (Fig. 9).

According to Table 5 the TiCN formation in composition II leads to improved oxidation resistance in comparison to composition I with the Al addition, compare Figs. 10 and 11. The state

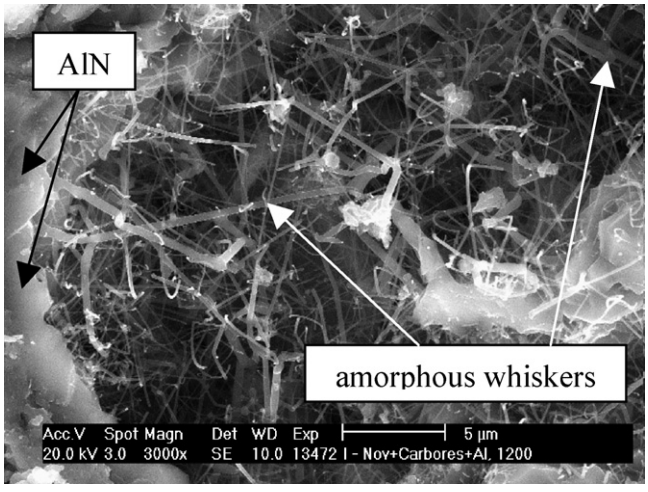

Fig. 3. Model-composition I, magnification 3000×, coked at 1200 °C in air and sealed by carbon in an alumina crucible, whiskers based on Al_4C_3 and Al_2OC and amorphous whiskers containing Al, C, O in the previous position of aluminium grains, at the interface carbon matrix/aluminium grain a mostly dense AlN layer.

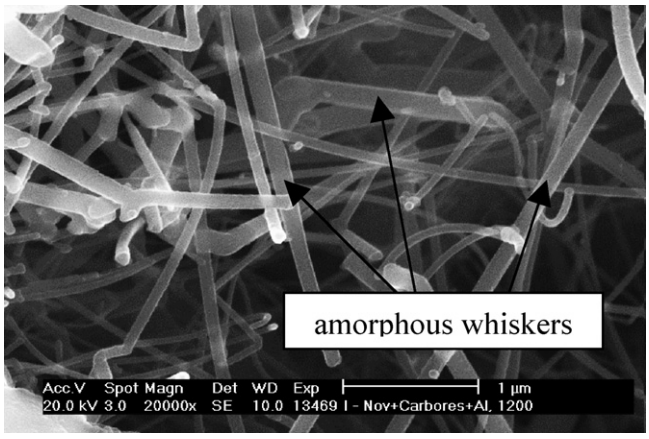

Fig. 4. Model-composition I, magnification 20,000×, coked at 1200 °C in air and sealed by carbon in an alumina crucible, mostly amorphous whiskers containing Al, C, O in the previous position of aluminium grains.

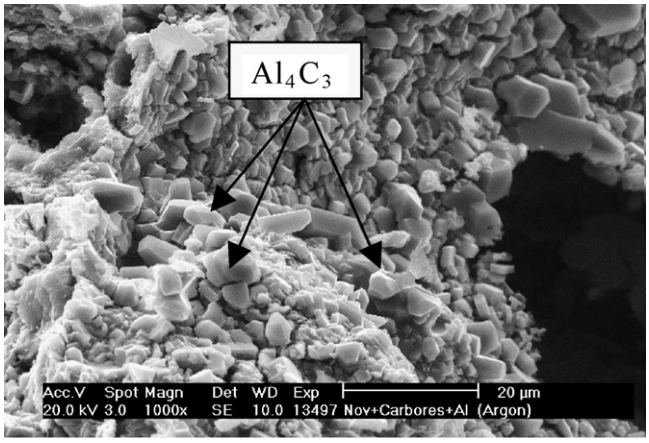

Fig. 5. Model-composition I, magnification 1000×, coked at 1000 °C in argon and sealed by carbon in an alumina crucible, Al_4C_3 crystal grains are formed.

of the art is the addition of aluminium. This addition leads to the formation of mostly amorphous whiskers at elevated temperatures that inhibit the oxidation. But the amorphous whiskers are not so sufficient as the crystalline TiCN. Composition III exhibits a remarkable oxidation resistance. The cubic TiC and

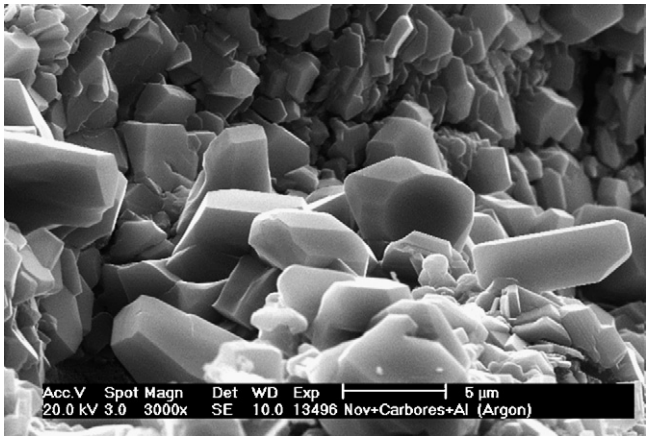

Fig. 6. Model-composition I, magnification 3000×, coked at 1000 °C in argon and sealed by carbon in an alumina crucible, Al_4C_3 crystal grains are formed.

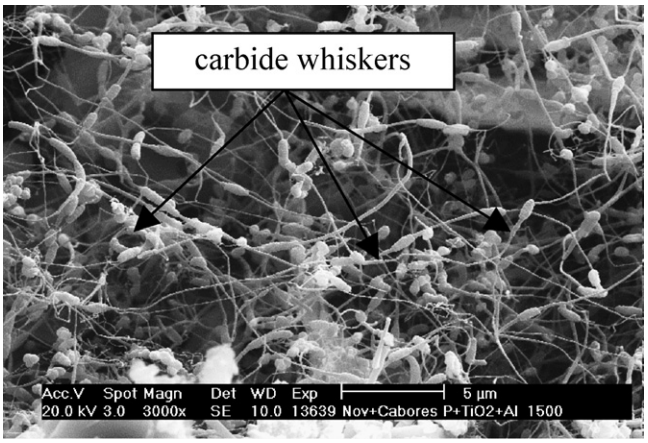

Fig. 7. Model-composition III, magnification 3000×, coked at 1500 °C in air and sealed by carbon in an alumina crucible, whiskers based on Al_2OC, Al_4O_4C and Al_4C_3.

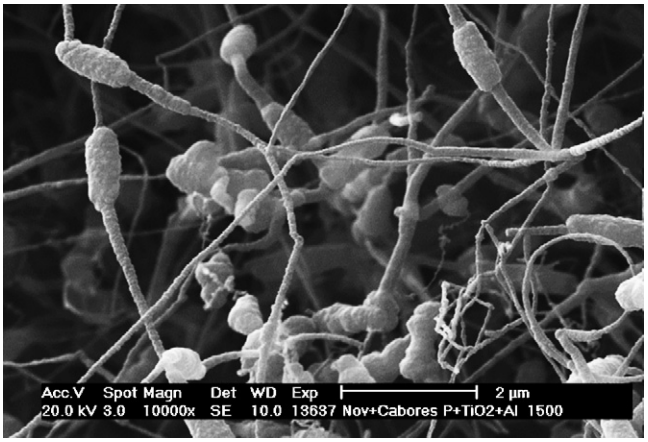

Fig. 8. Model-composition III, magnification 10,000×, coked at 1500 °C in air and sealed by carbon in an alumina crucible, whiskers based on Al_2OC, Al_4O_4C and Al_4C_3.

the crystalline Al_4C_3, Al_2OC and Al_4O_4C whiskers are mainly responsible for such a performance. In addition composition III presents approximately 30% higher cold compression strength. It is assumed that the dumbbell-shaped crystalline whiskers con-

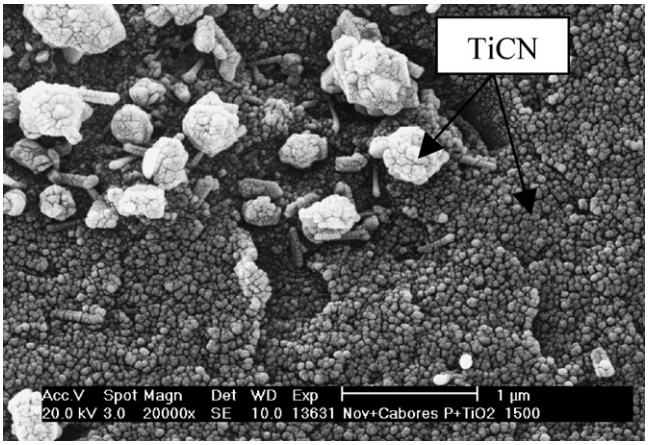

Fig. 9. Model-composition II, coked at 1500 °C in air and sealed by carbon in an alumina crucible, TiCN grains and TiCN agglomerates.

Table 5
Open porosity, cold compression strength (CCS) and oxidation depth of compositions I, II and III

	Composition I	Composition II	Composition III
Open porosity (Vol.%)	13.05 ± 0.05	13.1 ± 0.05	11.3 ± 0.05
CCS (MPa)	22.1 ± 0.5	23.5 ± 0.5	32.2 ± 0.5
Oxidation depth (mm)	9 ± 1	3 ± 1	2 ± 1

tribute to a very tight composite bonding matrix. This extreme tight and very hard structure can also be identified after the oxidation tests. This correlates also with investigations of TiC- and TiCN-coating materials as they are applied on metallic substrates for improved abrasion resistance of working tools.[13] Composition II and III present a very strong coherence between the MgO grains and the bonding matrix also after the oxidation test. In contrast, the structure of composition I without any Al additions is very weak and the abrasion resistance is very low.

It is assumed that samples coked at temperatures above 1300 °C would exhibit superior mechanical, thermal and chemical properties because of a high formation of TiCN and TiC in the compositions II and III. According to industrial applications,

Fig. 10. Oxidation tests at 1200 °C for 3 h in air of MgO–C samples coked at 1000 °C in air and sealed by carbon in an alumina crucible, left with Al-additions, right no Al-additions.

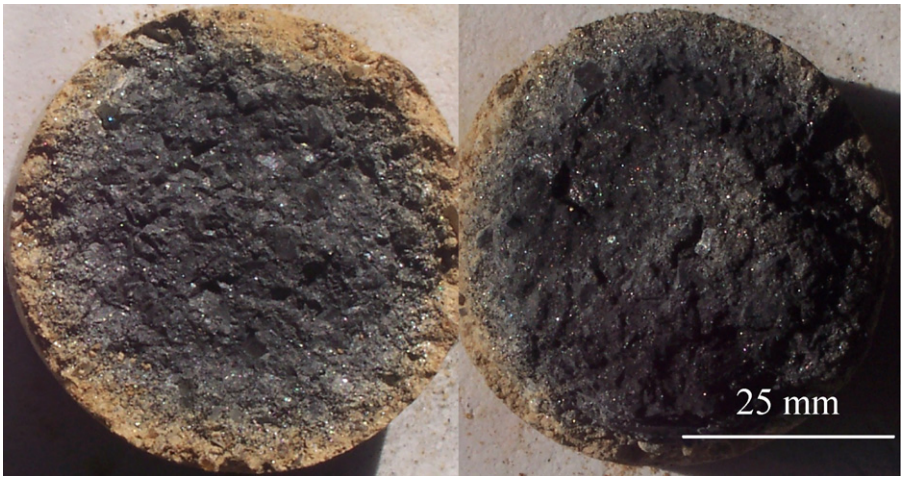

Fig. 11. Oxidation tests at 1200 °C for 3 h in air of MgO–C samples coked at 1000 °C in air and sealed by carbon in an alumina crucible, left TiO_2-additions, right TiO_2/Al-additions.

composition II and especially composition III posses superior performance to resist the hard service conditions such as abrasion, erosion and corrosion by metal/slag-melts as well as withstand thermal shock attacks. With respect to their extraordinary properties by low cost TiO_2-additions the model-compositions II and III can also be applied in the Al_2O_3–ZrO_2–C system for the development of submerged entry nozzles and sliding gates.

4. Conclusions

The addition of TiO_2 and TiO_2/Al in carbon bonded refractories leads to the formation of TiCN and TiC, respectively. These carbides improve the oxidation resistance, the mechanical strength as well as the abrasion resistance of the bonding matrix. In addition TiO_2 in carbon-bonded refractories with Al as an antioxidant, contributes to the formation of mainly crystalline Al_4C_3, Al_2OC and Al_4O_4C dumbbell shaped whiskers. These whiskers present a higher oxidation resistance in comparison to amorphous whiskers containing Al, C and O and it is assumed that they increase the thermal shock performance because of interlocking mechanisms in the bonding matrix. AlN is identified only at the interface carbon matrix/Al-grain. The whiskers in the previous position of Al grains contain only Al, O and C.

Acknowledgement

The authors would like to thank Dr. B. Ullrich for providing SEM analysis.

References

1. Aneziris, C. G., Borzov, D. and Ulbricht, J., Magnesia carbon bricks—a high duty refractory material. *Interceram. Refract. Man.*, 2003, 22–27.
2. Aneziris, C. G., Homola, F. and Borzov, D., Materials and process development of advanced carbon refractories for innovative metal processing. *Adv. Eng. Mater.*, 2004, **6**, 562–568.
3. Buchebner, G., Sampayo, L. and Samm, V. Development, production and application of pitch bonded magnesia carbon bricks with respect to their improved environmental compatibility. In 47th International Colloquium on Refractories, Aachen, 2004, p. 42–45.
4. Boenigk, W., Stiegert, J., Jacob, Ch., Schnitzler, D., Aneziris, C. G., Borzov, D., *et al*. MgO–C-bricks produced in a cold-mixing process using a graphite forming binder system. In 47th International Colloquium on Refractories, Aachen, 2004, p. 46–51.
5. Aneziris, C. G., Li, Y. W., Li, N. and Hampel, M., Physical and mechanical properties of environmental friendly carbon-bonded Al_2O_3–C-refractories for sliding gate applications. *cfi/Ber. DKG 82*, 2005, **9**, E1–E5.
6. Lee, W. E. and Zhang, S., Melt corrosion of oxide and oxide-carbon refractories. *Int. Mat. Rew.*, 1999, **44**(3), 77–104.
7. Yamakuchi, A., Behaviors of SiC and Al added to carbon-containing refractories. *Taikabutsu Overseas*, 1999, **4**, 14–18.
8. Watanabe, A., Takahashi, H. and Taganaga, S., Behavior of different metals added to MgO–C bricks. *Taikabutsu Overseas*, 1987, **7**, 17–23.
9. Zhang, S., Marriott, N. J. and Lee, W. E., Thermochemistry and microstructures of MgO–C refractories containing various antioxidants. *J. Eur. Ceram. Soc.*, 2001, **21**, 1037–1047.
10. Lee, J. W. and Duh, J. G., High temperature MgO–C–Al refractories-metal reactions in high aluminum-content alloy steels. *J. Mater. Res.*, 2003, **18**, 1950–1958.
11. Yamaguchi, A., Zhang, S. and Yu, J., Effect of refractory oxides on the oxidation of graphite and amorphous carbon. *J. Am. Ceram. Soc.*, 1996, **79**, 2509–2511.
12. Li, Y. W., Aneziris, C. G., Yi, X. X., Jin, S. L. and Li, N., Formation of dumbbell-shaped β-SiC whiskers in Al_2O_3–ZrO_2–C composite refractories. *Interceram. Refract. Man.*, 2005, 20–23.
13. Guemmaz, M., Moraitis, G., Mosser, A., Khan, M. A. and Parlebas, J. C., Band structure of substoichiometric titanium nitrides and carbonitrides: spectroscopical and theoretical investigations. *J. Phys. Condens. Matter*, 1997, **9**, 8453–8463.